Vascular endothelial platelet endothelial cell adhesion molecule 1 (PECAM-1) regulates advanced metastatic progression

Horace DeLisser[a,1], Yong Liu[b,1], Pierre-Yves Desprez[b], Ann Thor[c], Paraskevei Briasouli[b], Chakrapong Handumrongkul[b], Jonathon Wilfong[b], Garret Yount[b], Mehdi Nosrati[d,2], Sylvia Fong[b,3], Emma Shtivelman[b,3], Melane Fehrenbach[a], Gaoyuan Cao[a], Dan H. Moore[b], Shruti Nayak[b], Denny Liggitt[e], Mohammed Kashani-Sabet[d,2], and Robert Debs[b,4]

[a]Department of Medicine, University of Pennsylvania Medical Center, Philadelphia, PA 19104; [b]California Pacific Medical Center Research Institute, San Francisco, CA, 94107; [c]Department of Pathology, University of Colorado, Denver School of Medicine, Aurora, CO 80045; [d]Auerback Melanoma Research Laboratory, University of California San Francisco Cancer Center, University of California, San Francisco, CA 94143; and [e]Department of Comparative Medicine, University of Washington School of Medicine, Seattle, WA 98195

Edited* by James E. Cleaver, University of California, San Francisco, CA, and approved August 17, 2010 (received for review April 7, 2010)

Most patients who die from cancer succumb to treatment-refractory advanced metastatic progression. Although the early stages of tumor metastasis result in the formation of clinically silent micrometastatic foci, its later stages primarily reflect the progressive, organ-destructive growth of already advanced metastases. Early-stage metastasis is regulated by multiple factors within tumor cells as well as by the tumor microenvironment (TME). In contrast, the molecular determinants that control advanced metastatic progression remain essentially uncharacterized, precluding the development of therapies targeted against it. Here we show that the TME, functioning in part through platelet endothelial cell adhesion molecule 1 (PECAM-1), drives advanced metastatic progression and is essential for progression through its preterminal end stage. PECAM-1–KO and chimeric mice revealed that its metastasis-promoting effects are mediated specifically through vascular endothelial cell (VEC) PECAM-1. Anti–PECAM-1 mAb therapy suppresses both end-stage metastatic progression and tumor-induced cachexia in tumor-bearing mice. It reduces proliferation, but not angiogenesis or apoptosis, within advanced tumor metastases. Because its antimetastatic effects are mediated by binding to VEC rather than to tumor cells, anti–PECAM-1 mAb appears to act independently of tumor type. A modified 3D coculture assay showed that anti–PECAM-1 mAb inhibits the proliferation of PECAM-1–negative tumor cells by altering the concentrations of secreted factors. Our studies indicate that a complex interplay between elements of the TME and advanced tumor metastases directs end-stage metastatic progression. They also suggest that some therapeutic interventions may target late-stage metastases specifically. mAb-based targeting of PECAM-1 represents a TME-targeted therapeutic approach that suppresses the end stages of metastatic progression, until now a refractory clinical entity.

metastasis | endothelium | tumor microenvironment

Tumor metastasis requires that a number of sequential steps, including tumor cell invasion, intravasation, homing, extravasation, tumor neoangiogenesis, and proliferation, each be completed successfully (1–4). Thus, tumor metastasis comprises semidiscrete stages, in part driven by distinct cellular events. The tumor microenvironment (TME), both via direct interactions with tumor cells and through paracrine-based signaling, plays an important role in controlling the early stages of metastatic spread (2–4). In contrast, factors that drive the progression of tumor metastases to a life-threatening, preterminal stage are poorly understood. As in earlier stages, they likely involve molecular signaling between malignant cells and their macro- and microenvironments (1, 5, 6).

Advanced metastatic progression causes death in most patients who die from cancer. However, in preclinical models, novel interventions generally are tested directly against locally injected tumors or against early-stage, micrometastatic spread. In contrast, models specifically examining the effects of interventions against the late stages of metastatic progression (the lethal, organ-destructive growth of already advanced metastases) are rarely studied. Antitumor interventions administered during the advanced stages of metastatic progression typically are both ineffective and poorly tolerated. Indeed, key events that define the early stages of metastatic spread may differ from those driving advanced metastatic progression. We hypothesized that testing novel interventions against the early stages of metastatic spread may fail to identify critical factors that selectively regulate the progressive growth of already advanced tumor metastases. Therefore, our studies focused on models assessing the progression of already well-established tumor metastases rather than on models assessing the early stages of metastatic spread.

Platelet endothelial cell adhesion molecule 1 (PECAM-1) is a 130-kDa cell surface protein of the Ig-like superfamily, with six Ig-like domains in the extracellular domain. It is expressed on certain WBC, platelets, and vascular endothelial cells (VEC) and interacts homophilically with itself or heterophilically with putative ligands to tranduce downstream inhibitory signals via its cytoplasmic domain (7, 8). PECAM-1 is involved in a number of processes relevant to growth and the spread of primary tumors, including angiogenesis, vascular permeability, and leukocyte trafficking out of the circulation (9, 10). In addition, earlier studies have shown that systemic delivery of an anti–PECAM-1 ribozyme suppresses the progression of already established tumor metastases (11). We assessed the potential role of PECAM-1 in regulating late-stage metastatic progression. Here, we provide evidence that VEC PECAM-1 regulates proliferation in advanced tumor metastases, independent of its activity as a mediator of angiogenesis. Importantly, anti–PECAM-1 mAb demonstrates potent antimetastatic effects specifically against the lethal preterminal stage of metastatic progression.

Results

Anti–PECAM-1 mAb Inhibits Late-Stage but Not Early-Stage Metastatic Tumor Progression in the Lung. Several aggressively metastatic tumor cell lines, including murine B16-F10 melanoma, 4T1

Author contributions: H.D., P.-Y.D., A.T., P.B., G.Y., D.L., M.K.-S., and R.D. designed research; H.D., Y.L., P.-Y.D., A.T., P.B., C.H., J.W., G.Y., M.N., S.F., E.S., M.F., G.C., D.L., M.K.-S., and R.D. performed research; H.D. contributed new reagents/analytic tools; H.D., Y.L., P.-Y.D., A.T., P.B., C.H., J.W., G.Y., M.N., S.F., E.S., M.F., G.C., D.H.M., S.N., D.L., M.K.-S., and R.D. analyzed data; and H.D., P.-Y.D., A.T., G.Y., S.F., E.S., D.H.M., D.L., M.K.-S., and R.D. wrote the paper.

Conflict of interest statement: H.D., D.L., M.K.-S., and R.D. have financial ownership of Genomic Systems, LLC, an entity that provided partial funding for this work.

*This Direct Submission article had a prearranged editor.

Freely available online through the PNAS open access option.

[1]H.D. and Y.L. contributed equally to this work.

[2]Present address: California Pacific Medical Center Research Institute, San Francisco, CA 94107.

[3]Present address: Bionovo Inc., Emeryville, CA 94608.

[4]To whom correspondence should be addressed. E-mail: debs@cpmcri.org.

This article contains supporting information online at www.pnas.org/lookup/suppl/doi:10.1073/pnas.1004654107/-/DCSupplemental.

mammary carcinoma, and LOX human melanoma, were evaluated. In particular, i.v. injected B16-F10 cells yield highly reproducible numbers of tumor metastases in the lung as well as in extrapulmonary organs, including the ovaries (12). From days 0–7 following i.v. injection (early-stage metastasis), most B16-F10 lung metastases remain small clusters containing <10 cells each. In contrast, by days 12–14 (late-stage metastasis), >35% of metastases are already >3 mm in diameter (5). We used mAb 390, a bioactive anti-murine PECAM-1 mAb (13), which specifically binds to an epitope within a 14-aa sequence of the second Ig-like domain of mouse PECAM-1. mAb390 binds to murine VEC but does not bind to murine or human tumors (13). Furthermore, it does not directly inhibit tumor cell proliferation, alter tumor cell adhesion to VEC or to platelets, or affect the transendothelial migration of tumor cells (Fig. S1 *A–E*). To target early- versus late-stage metastasis selectively, five i.v. doses of mAb 390 or isotype-control mAb were administered either 0–7 or 7–15 d after B16-F10 cell injection. Anti–PECAM-1 mAb significantly ($P < 0.0001$) decreased late-stage but did not affect early-stage tumor metastases (Fig. 1 *A* and *B*). The late-stage–specific anti-metastatic effects produced by mAb 390 are consistent with its inability to inhibit either tumor cell–platelet or tumor–endothelial cell interactions (Fig. S1 *C–E*), processes involved in the initial establishment of distant metastatic tumor foci. Systemic anti–PECAM-1 mAb also significantly reduced the late-stage metastatic progression of two other aggressively metastatic tumor lines, murine 4T1 mammary carcinoma ($P < 0.0001$) (Fig. 1*C*) and human LOX melanoma xenograft tumors ($P < 0.005$) (Fig. 1*D*), demonstrating that anti–PECAM-1 mAb therapy can suppress the late-stage metastatic progression of solid tumor types of different tissue origin. Anti–PECAM-1 mAb 390 has been shown to inhibit PECAM-1–dependent activities specifically and functions in a manner similar to a number of other anti–PECAM-1 antibodies (which bind to epitopes distinct from mAb 390), in a number of in vitro and in vivo assays (8, 14–16).

Enhanced Effectiveness of Anti–PECAM-1 mAb Against Preterminal Metastatic Disease. We next tested anti–PECAM-1 mAb 390 specifically against the preterminal stage of metastatic progression. We assessed the effects of administering one additional preterminal dose (a sixth mAb dose) to mice already severely ill from extensive B16-F10 tumor metastases. This preterminal anti–PECAM-1 mAb dose significantly reduced the percentage of lung occupied by tumor metastases [control group: 34.3 ± 4.2%, standard five-dose mAb 390 group: 19.6 ± 4.2% ($P < 0.05$ versus control); extended six-dose group: 9.0 ± 3.3% ($P < 0.0001$ versus control; $P < 0.05$ versus five-dose group)] (Fig. 2 *A* and *B*). It also reduced ($P < 0.001$) ovarian metastases (Fig. 2*C*), indicating that anti–PECAM-1 mAb therapy is systemically active. The preterminal (sixth mAb) dose also increased total body weight, determined at the time of sacrifice ($P < 0.0005$), when compared with either mice not receiving the preterminal anti-PECAM-1-mAb dose or control groups (Fig. 2*D*). Concurrently, lung tumor weights were significantly reduced in the group receiving the preterminal dose, showing that the preterminal dose better preserved normal body weight. These results indicate that targeting PECAM-1 reduces tumor-induced cachexia. Similarly, a preterminal dose of anti–PECAM-1 mAb 390 also significantly increased antimetastatic efficacy against highly advanced 4T1 metastases (Fig. 2*E*).

Anti–PECAM-1 Antibody Inhibits Tumor Cell Proliferation but Not Apoptosis or Angiogenesis. To identify pathway(s) through which anti–PECAM-1 mAb suppresses preterminal metastatic progression, its effects on tumor proliferative, apoptotic, and angiogenic rates were measured (Table 1). Tumor angiogenic rates were assessed by immunoreactivity to anti-von Willibrand factor (17) and to CD34 (to assess immature angiogenic endothelium) (18–20). Angiogenic and apoptotic (17) rates were comparable. However, the preterminal anti–PECAM-1 mAb dose reduced tumor cell proliferation (21) in highly advanced B16-F10 ($P < 0.005$) tumor metastases. Thus, although anti–PECAM-1 mAb 390 reduces angiogenesis within primary s.c. tumors (13), it specifically suppresses proliferation but has no affect on angiogenesis within advanced tumor metastases. As Fig. 2*A* illustrates, tumor metastases increase in size rapidly during the very late stages of metastatic progression, indicating that these tumor cells are proliferating rapidly. A single additional dose of anti–PECAM-1 mAb administered when metastases are both highly advanced and rapidly proliferating effectively suppressed proliferation. Suppression of proliferation within advanced metastases by the preterminal anti–PECAM-1 mAb dose at least in part explains its marked reduction of advanced metastatic burden.

Decreased Lung Metastases in PECAM-1–KO Mice. Because B16-F10 tumor cells are syngeneic with PECAM-1–KO mice (22), the effects of PECAM-1 on the metastatic progression of B16-F10 also can be studied in KO versus WT mice. Therefore, the development of lung metastases following tail vein injection of B16-F10 cells into WT versus PECAM-1–KO mice was assessed (22). Visible lung metastases were not detected in either WT or KO mice 7 d after tumor cell injection (Fig. 3*A*). However, from days 10–16 after tumor cell injection, the number of metastatic lung tumors (Figs. 3 *A* and *B* and 4 *A* and *C*), as well as lung weight (Fig. 4*E*), was markedly reduced in KO versus WT mice. Even more striking suppression was observed in the size of tumor nodules. Suppression of metastatic tumors also was

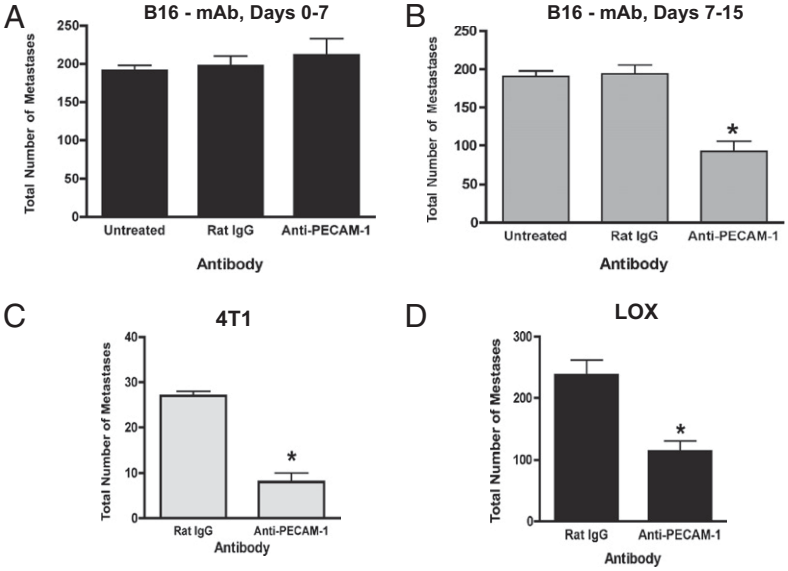

Fig. 1. Anti–PECAM-1 mAb specifically suppresses late-stage but not early-stage metastatic progression. (*A* and *B*) Groups of C57BL/6 mice received 25,000 B16-F10 cells i.v. (day 0). (*A*) In groups receiving early-stage treatment, each mouse received one i.v. injection of 200 μg of anti–PECAM-1 mAb or isotype-control mAb on day 0 and subsequently received one mAb dose every other day through day 7 (five mAb doses). (*B*) In groups receiving late-stage treatment, each mouse received one i.v. injection of 200 μg anti–PECAM-1 or isotype control mAb on day 7 and subsequently received one dose every other day through day 15 (five mAb doses). All mice were euthanized when multiple control mice became moribund. (*C*) BALB/c mice received 25,000 4T1 cells i.v. (*D*) BALB/c nude mice received 1×10^6 LOX cells i.v. Mice received five anti–PECAM-1 or control mAb doses from days 7–15 as above. When multiple control mice became moribund, all mice were euthanized and analyzed. Values represent the mean number of lung metastases ± SEM per mouse ($n = 10$). Potential statistical significance of differences for *A–D* was assessed using pairwise two-sided Student's *t* tests. *$P < 0.05$.

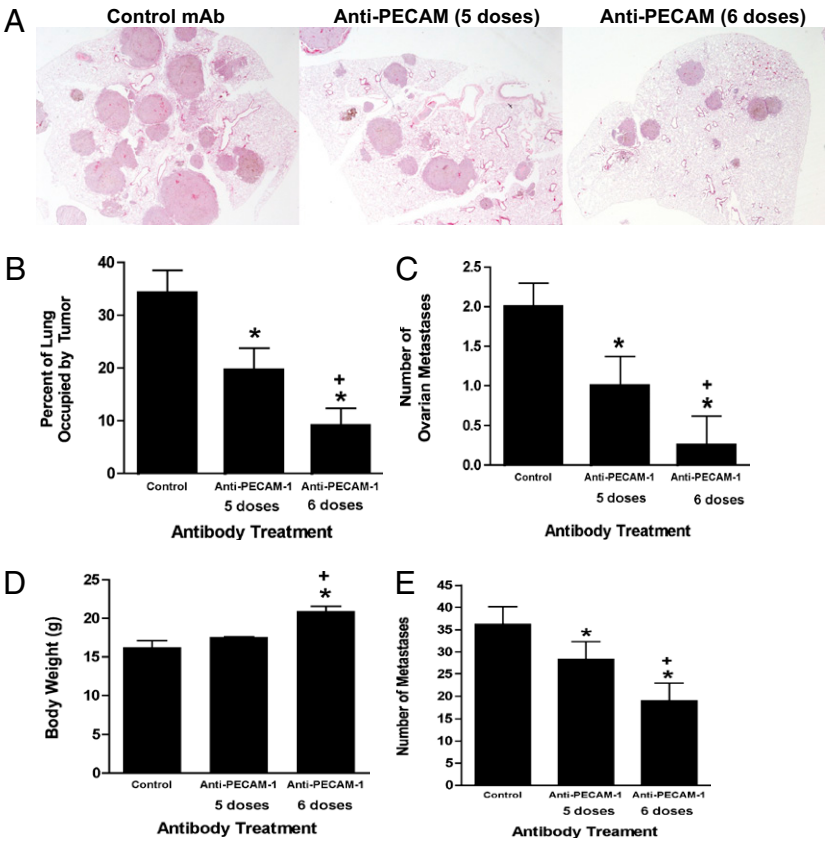

Fig. 2. Preterminal administration of anti–PECAM-1 mAb is highly effective against end-stage metastatic progression. C57BL/6 mice received B16-F10 cells and then five doses (last dose on day 15) or six doses (last dose on day 18) of anti–PECAM-1 or isotype control mAb. All mice were euthanized when multiple control mice became moribund. (*A*) Representative lung sections from mice treated with control mAb and mice treated with five or six doses of anti–PECAM-1 mAb. Metastases stain grayish-red. (*B*) Percent lung area occupied by B16-F10 melanoma. There were significant differences among the three treatments ($P = 0.001$ by Kruskal–Wallis rank test). Also, all pairwise comparisons were significantly different: five doses vs. none, $P = 0.02$; six doses vs. none, $P = 0.002$; and five doses vs. six doses, $P = 0.02$; all pairwise tests were by Mann–Whitney rank test. (*C*) Mean number of B16-F10 ovarian metastases. (*D*) Mean body weight of animals. There were significant differences among the three treatments ($P = 0.002$ by Kruskal–Wallis rank test). Also, six doses vs. none ($P = 0.003$) and five doses vs. six doses ($P = 0.004$) were significantly different. All pairwise tests were by Mann–Whitney rank test. (*E*) BALB/c mice received 25,000 4T1 cells i.v. and then received five doses (last dose on day 15) or six doses (last dose on day 18) of anti–PECAM-1 or isotype control mAb. All mice were euthanized when multiple control mice became moribund. Values represent mean ± SEM ($n = 10$). In *C* and *E*, potential statistical significance of differences was assessed using pairwise two-sided Student's *t* tests. $^{*}P < 0.05$ vs. control; $^{+}P < 0.05$ vs. five doses.

demonstrated in the lungs of KO animals by H&E staining of lungs harvested 15 d after tumor cell injection (Fig. 3*B*). Because anti–PECAM-1 mAb was effective against late- but not against early-stage metastases (Fig. 1 *A* and *B*), we then assessed more precisely whether early-stage metastatic progression was affected in PECAM-1–KO mice. To determine whether the early stages of metastatic spread are controlled differently in PECAM-1–KO versus WT mice, H&E staining was performed on lung tissue obtained at a much earlier time point, 4 d after i.v. injection of B16-F10 tumor cells. Subclinical lesions (<10 cells) detected in the walls of the alveoli at day 4 (Fig. 3*D*) were similar in number and size in WT and PECAM-1–KO mice (Table S1). Unlike the marked differences between WT and KO mice in the number and size of large, macroscopic B16-F10 metastases (Fig. 3 *A* and *B*), numbers of micrometastatic foci were comparable in WT and KO mice (Table S1). Therefore, advanced metastatic progression, but not the early stages of metastatic spread, is suppressed in both PECAM-1–KO mice and WT mice receiving anti–PECAM-1 mAb. Taken together, these data indicate that PECAM-1 plays an important role in regulating the progression of established metastases from subclinical metastatic lesions to macroscopic, life-threatening tumor metastases. However, PECAM-1 appears uninvolved in controlling the initial establishment of metastatic tumor foci or in mediating the passage of primary tumor cells across the vascular endothelium (Fig. S1 *C–E*), events critical to spread from the primary tumor itself.

Reconstitution of PECAM-1–Null Mice with Bone Marrow from WT Mice Does Not Restore the WT Phenotype. Anti–PECAM-1 mAb 390 does not bind to tumor cells either in culture (Fig. S1*A*) or in tumor-bearing mice (13) whose late-stage metastases it suppressed. Furthermore, it does not directly inhibit tumor cell proliferation in vitro (Fig. S1*B*). To determine whether PECAM-1 expressed on VEC and/or bone marrow-derived WBC mediates its prometastatic effects, chimeric mice were generated by reconstituting WT mice with KO marrow (PECAM-1–positive VEC/PECAM-1–negative platelets WBC, designated WT_{EC}-KO_{BM}) or by reconstituting KO mice with WT marrow (PECAM-1–negative endothelium/PECAM-1–positive platelets WBC, designated KO_{EC}-WT_{BM}) (23). Reconstitution of WT animals with KO marrow did not suppress the development of metastases, and reconstitution of KO mice with marrow from WT mice did not restore the WT, prometastatic phenotype (Fig. 4 *A–E*). These data indicate that the antimetastatic

Table 1. Extended anti–PECAM-1 mAb therapy significantly reduces tumor mitotic rates, but not tumor angiogenic or tumor apoptotic rates in mice bearing advanced tumor metastases

B16-F10 tumors	Tumor angiogenesis	Tumor apoptosis*	Tumor mitosis†
Anti–PECAM-1 mAb-treated			
	10.6 ± 1.7‡	9.0 ± 3.4	14.4 ± 1.6¶
	209.7 ± 44.0§		
Control mAb-treated			
	11.3 ± 2.6‡	10.8 ± 4.0	21.5 ± 1.7
	191.7 ± 45.9§		

Mice bearing metastatic B16-F10 or 4T1 tumors were treated with six doses of either anti–PECAM-1 or control mAb and were euthanized as described in Fig. 1. Tumor-bearing lungs were removed and processed, and tumor angiogenic, mitotic, and apoptotic rates were measured as described in *Materials and Methods*. The lack of difference in tumor angiogenic rates between groups was confirmed by assessing immunoreactivity to CD34. Potential statistical significance of differences was assessed using an unpaired two-tailed Student *t* test ($P < 0.05$ vs. control).

*Tumor apoptotic rates were measured as described in *Materials and Methods*.

†Tumor mitosis counts were measured by immunoreactivity to Ki67 (19).

‡Tumor angiogenic rates measured by immunoreactivity to factor VIII-VWF (17).

¶Potential statistical significance of differences was assessed using a pairwise two-sided Student's *t* test. $P < 0.005$ versus control; values are ± SD.

§Tumor angiogenic rates measured by immunoreactivity to CD34 (18).

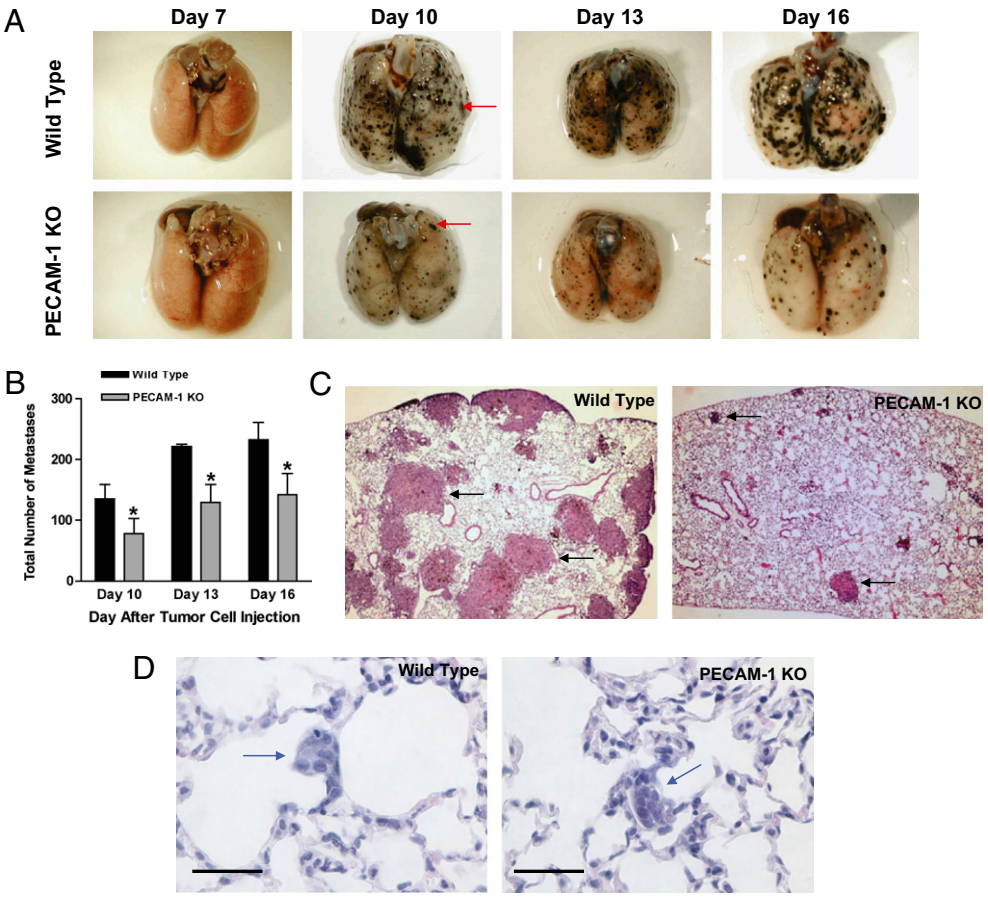

Fig. 3. Late-stage, but not early-stage, metastatic progression of B16-F10 melanoma tumors is suppressed in PECAM-1–KO mice versus WT. (*A*) Representative lungs obtained from WT and PECAM-1–KO animals 7, 10, 13, and 16 d after i.v. injection with B16-F10 melanoma cells. Tumor nodules are not observed on the surface of the lung 7 d after tumor injection, but are readily visible in both WT and PECAM-1–KO mice by day 10 (red arrows). At all time points assessed after day 7, progression of the size and number of tumor metastases was significantly suppressed in PECAM-1–KO mice. (*B*) Mean number of tumor nodules visible on the surface of the right lung in WT and PECAM-1–KO mice on days 10, 13, and 16. At least 40 nodules were analyzed from three mice for each strain. Values are mean ± SEM ($n = 2$ or 3; $P < 0.001$; pairwise two-sided Student's t test). A marked suppression in the mean area of these nodules was observed in PECAM-1–KO mice (day 16: WT 1.14 vs. PECAM-1–KO 0.26 mm^2; $^*P < 0.05$ vs. WT). (*C*) H&E-stained lung tissues demonstrating large macroscopic nodules (black arrows) were greatly increased in number and size in the WT versus PECAM-1–KO mice, 15 d after tumor cell injection. (*D*) Small, subclinical lesions (<10 cells) detected in the walls of the alveoli (blue arrows) in lungs harvested 4 d following tumor cell injection. Unlike the marked differences in the number and size of large, macroscopic B16-F10 metastases in WT and PECAM-1–KO mice (*A* and *B*), the number and size of micrometastatic foci were comparable in WT and PECAM-1–KO mice (Table S1). (Scale bar: 50 μm.)

effects observed in PECAM-1–KO mice, and likely those produced by anti–PECAM-1 mAb 390, are mediated by blocking VEC PECAM-1.

PECAM-1–Dependent Paracrine Factors Regulate Tumor Proliferation. We developed a variant of a 3D coculture system as a model for tumor cell–VEC interactions within the tumor microenvironment. Tumor cells are added to capillary-like structures (CLS) of VEC already formed on a basement-membrane substrate. VEC do not divide once plated on Matrigel (24). Although these CLS typically regress within 24–36 h (24), adding tumor cells maintained CLS integrity for ≥5 d. Anti–PECAM-1 mAb, unlike control mAb, suppressed B16-F10 or 4T1 proliferation by 50–60% ($P < 0.05$) in this 3D coculture system (Fig. S2), thus accurately recapitulating the proliferation-suppressing phenotype it produced in tumor-bearing mice (Table 1). To assess whether PECAM-1 regulates proliferation via soluble mediators, B16-F10 cells were grown in conditioned medium from anti–PECAM-1– or control mAb-treated 3D cocultures. Anti–PECAM-1 mAb conditioned medium inhibited tumor cell proliferation by >60% (Movies S1 and S2), indicating that anti–PECAM-1 mAb-regulated paracrine factors mediate its ability to suppress tumor cell proliferation. Anti–PECAM-1 mAb 390 therapy also inhibits the growth of primary tumors that do not express PECAM-1 (13), consistent with its ability to act, at least in part, through its regulation of paracrine factors.

Lack of PECAM-1–Dependent Cellular Infiltration in Anti–PECAM-1–Treated Tumors. Multiple H&E-stained sections from metastatic tumors and surrounding tissues were examined to identify any characteristics that might differentiate anti–PECAM-1 mAb-treated mice from control mice. None were detected. Tumors were examined specifically for accumulations of F4/80 antigen-positive macrophages using immunohistochemistry (25). The presence of macrophages within individual tumor nodules varied from rare to moderate. However, neither the pattern nor the extent of macrophage infiltration differed between anti–PECAM-1 mAb-treated and control specimens (Fig. S3). Thus, although tumor-infiltrating macrophages may play a role in mediating the antimetastatic effects produced by anti–PECAM-1 mAb, these results suggest that this role is limited. This hypothesis is supported by results obtained in the 3D coculture assay (in which no macrophages were present), where anti–PECAM-1 mAb exerted antitumor and antiproliferative effects comparable to those it produced in tumor-bearing mice.

Discussion

Although rarely studied in preclinical models, advanced metastatic progression causes death in the great majority of patients who die from cancer. Although the early stages of tumor metastasis result in the formation of clinically silent micrometastatic foci (2, 4, 6), its advanced stages primarily reflect the progressive, organ-destructive growth of already well-established metastases (5). The molecular determinants that control the end stages of metastatic progression remain largely uncharacterized. Mechanistically, our results support the hypothesis that VEC PECAM-1–regulated paracrine factors drive the lethal progression of advanced tumor metastases. Anti–PECAM-1 mAb blocks this progression by altering the release of soluble factors that drive proliferation within these advanced metastases. This model is supported by each of the following observations. Anti–PECAM-1 mAb, even at very high concentrations, does not directly inhibit tumor cell proliferation in culture. In contrast, conditioned medium (which contains PECAM-1–regulated secreted factors) from mAb 390-treated, but not from isotype control mAb-treated, cocultures strongly inhibits tumor cell proliferation in culture. Furthermore, anti–PECAM-1

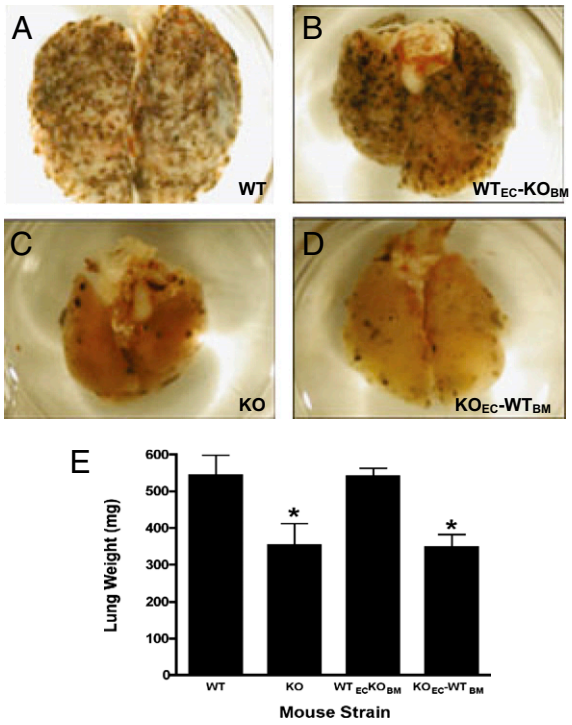

Fig. 4. Metastatic progression of B16-F10 melanoma tumors in reciprocal bone marrow chimeric mice reveals that VEC PECAM-1 mediates its prometastatic effects. Shown are lungs from animals injected with B16-F10 melanoma cells. The following animals were studied: (*A*) WT mice, (*B*) WT mice reconstituted with PECAM-1–KO marrow (WT$_{EC}$-KO$_{BM}$,), (*C*) PECAM-1–KO mice, and (*D*) PECAM-1–KO mice reconstituted with WT marrow (KO$_{EC}$-WT$_{BM}$). (*E*) Lung weights differed significantly among the four strains (*$P = 0.03$ by Kruskal–Wallis rank test). Lung weights were significantly decreased in the PECAM-1–KO mice and PECAM-1–KO mice reconstituted with WT marrow. Lung weights were significantly reduced in the KO mice and KO mice reconstituted with WT marrow vs. WT mice and WT mice reconstituted with KO marrow. Also, the pairs WT vs. KO and WT-KO vs. KO-WT differed significantly ($P = 0.0497$ and $P = 0.0463$, respectively, based on Mann–Whitney rank test). $n = 10$. Values are mean ± SEM.

mAb 390 does not bind to any of the tumor cell types whose metastasis it suppresses. Rather, the antimetastatic activity produced by anti–PECAM-1 mAb is mediated specifically by its binding to PECAM-1 expressed on VEC.

Intriguingly, we found that anti–PECAM-1 mAb suppressed tumor metastasis more effectively when administered at an advanced stage (Fig. 1*B*), a time when the explosive growth of macroscopic, already well-established metastases typically is seen (5). Conversely, administration of the antibody during the initial formation of micrometastatic tumor foci did not inhibit the emergence of clinically apparent metastases. In addition, late-stage tumor metastases were suppressed strongly, whereas early metastatic spread was unaffected in PECAM-1–KO versus WT mice. Chimeric mice revealed that the PECAM-1 metastasis-promoting effects are mediated by VEC-expressed, not by WBC-expressed, PECAM-1. Because its antimetastatic effects are mediated by binding to VEC rather than the tumor cells themselves, anti–PECAM-1 mAb appears to act independent of tumor type.

Single-agent anti–PECAM-1 mAb is highly effective against advanced, life-threatening tumor metastases but is ineffective against clinically silent micrometastases. Our results demonstrate that an anticancer treatment can effectively treat the preterminal stages of metastatic progression, but be ineffective when administered during its early, asymptomatic stages. In contrast, the currently used antitumor mAbs are being used increasingly to treat earlier-stage human cancers (6, 26). Furthermore, PECAM-1 acts through VEC to regulate metastasis in a novel way, by specifically controlling proliferation, not angiogenesis, in advanced tumor metastases. Targeted VEGF antagonists inhibit angiogenesis in both primary and metastatic tumors and play a major role in treating metastatic human cancers (27). Anti–PECAM-1 mAb inhibits angiogenesis in primary tumors (13) but does not affect angiogenesis within advanced tumor metastases, indicating that some molecularly targeted therapies can elicit different biologic responses within different tumor microenvironments. Thus, the vascular endothelium, acting through VEGF, as well as PECAM-1, can regulate metastatic progression through different mechanisms, further expanding its role in directing tumor metastasis.

Remarkably, dose-intensive, preterminal mAb administration effectively treated the treatment-refractory end stages of metastatic progression. Specifically, one additional (sixth) dose of anti–PECAM-1 mAb, administered to mice that were already preterminal, was itself strikingly effective, further reducing lung metastatic burden by an additional 50% against B16-F10 and an additional 35% against 4T1 tumors, when compared to the five anti-PECAM-1-mAb dose regimen lacking a pre-terminal dose. Although many anticancer treatments are significantly more toxic in hosts already debilitated from advanced tumor metastases, high doses of anti–PECAM-1 mAb administered during the preterminal phase not only appeared nontoxic but also significantly reduced tumor-induced cachexia. In addition, PECAM-1–KO mice grow and develop normally (22). Taken together, these results suggest anti-PECAM mAb therapy may be well tolerated, even in human patients already severely debilitated by advanced metastases.

Studies of metastasis often focus on the early stages of metastatic spread, and the study of preterminal metastatic progression generally has been avoided. In contrast, clinical trials of investigational anticancer agents, selected based on early-stage preclinical studies, often are conducted in patients bearing late-stage metastases, suggesting a mismatch between models studied and patients treated. The striking efficacy of anti–PECAM-1 mAb against preterminal metastases coupled with its inactivity against very early-stage metastatic spread suggests that the lethal growth of advanced tumor metastases is controlled, at least in part, by late-stage–specific, prometastatic drivers. Furthermore, these results indicate that late-stage–specific testing of novel antitumor agents will reveal some agents active only during this usually treatment-resistant phase of metastatic progression. Such agents may include agents previously determined to be ineffective when tested solely against early-stage metastatic spread.

This apparent anomaly may result in part from the largely proliferation-driven nature of advanced metastatic disease (5). Conversely, the successful establishment of micrometastatic foci depends upon the abilities of tumor cells to invade locally, intravasate home to distant organs, extravasate, and induce tumor neoangiogenesis (4). Recent studies have shown that i.v. injected nontumorigenic mammary gland cells can colonize and grow within the lung for prolonged periods (28), further supporting the concept that early metastatic spread occurs by a series of discrete stages. Taken together, our studies indicate that a complex interplay between elements of the TME, paracrine factors, and advanced tumor metastases controls the lethal progression of advanced tumor metastases. Selectively targeting PECAM-1 represents a TME-targeted therapeutic approach that suppresses even lethal, end-stage metastatic progression, until now a refractory clinical entity.

Materials and Methods

Monoclonal Antibodies. Anti–PECAM-1 mAb 390 is an IgG2A class anti-murine CD31 antibody that binds to a 14-aa epitope on domain II of the extracellular Ig domains of CD31 (6). An IgG2A rat isotype control mAb was purchased from Sigma. mAbs were cleared of LPS using the EndoTrap Red system (Lonza) to fewer than two units of endotoxin per milliliter as determined by a limulus amebocyte lysate assay (Pyrogent Plus; Lonza).

3D Coculture Assay. Six-well polystyrene plates (Corning) were coated with 300 μL of Matrigel (BD Biosciences). One hour later, 2×10^5 CD3 or H5V cells (VEC lines) were plated. Eight hours later, after VEC capillary-like structures had formed, 2×10^5 B16-F10 or 4T1 cells were added, together with 200 μg/mL of either anti–PECAM-1 or control mAb. mAbs were added again at 24 and 48 h, and all cells and culture supernatants for conditioned media were harvested at 72 h. All wells were trypsinized and counted using a hemocytometer.

In Vivo Monoclonal Antibody Treatments and Analysis of Antitumor Activity. B16-F10 murine melanoma cells, LOX human melanoma cells, and 4T1 breast carcinoma cells were freshly thawed and grown in 10% FBS in RPMI-1640 medium (Invitrogen) for 48 h. On day 0, groups of 6-wk-old female C57BL/6 (B16-F10), BALB/C (4T1), or BALB/C nude (LOX) mice (n = 10 mice per group) (Simonsen Laboratories) were injected i.v. with 25,000 B16-F10 cells, 50,000 4T1 cells, or 1,000,000 LOX cells, respectively, in 200 μL of culture medium. In groups receiving early-stage treatment, each mouse received one i.v. injection of 200 μg of anti–PECAM-1 mAb 390 or isotype control mAb on day 0 and one dose every other day through day 7. The groups receiving late-stage treatment received one i.v. injection of 200 μg of anti–PECAM-1 or isotype-control mAb on day 7 and then every other day through day 15. All mice were weighed on day 0, before tumor cell injection, and then were randomized so that treated and control groups had comparable weights. The mice were weighed again before they were killed. Differences in mean total body weight represent those occurring over the entire 21-d duration of the experiment. All mice were killed humanely when multiple tumor-bearing control mice required sacrifice. Although survival studies could not be performed (in accordance with institutional animal-care guidelines), the lack of early deaths in the six-dose mAb-treated group suggests their survival would be prolonged. Lungs dissected from each mouse were weighed immediately. For B16-F10–inoculated mice, lungs were infused transtracheally with 5% neutral buffered formalin/PBS. For 4T1- and LOX-inoculated mice, lungs were infused with 15% India ink in Fekete's solution. Black-brown B16-F10 metastatic tumors and counterstained 4T1 and LOX tumors (white) were counted under a dissecting microscope.

Analysis of Lung Surface Area Occupied by Metastatic Tumors. Images of all histologic sections in the anti–PECAM-1 mAb and control groups were captured using a Nikon Digital Sight D5-U1 camera and Nikon 80i microscope. The total lung surface area and the surface area occupied by individual tumor masses within the lung were outlined using the area function of NIS-Elements Software (Nikon Instruments), and the percentage of lung occupied by tumor was calculated.

Generation of Mice Chimeric for CD31 on VEC and WBC. Bone marrow chimeric mice were generated as previously described (23). Within 24 h after irradiation, 5×10^6 cells of donor marrow obtained from nonirradiated mice were injected i.v. into irradiated recipient mice. Tumor cells were injected 4–6 wk after transplantation. Flow cytometry analysis of leukocytes using an anti-mouse PECAM-1 antibody confirmed the chimeric phenotype.

Immunohistochemistry. Antibodies used include rat anti-murine K_i-67 antigen and rabbit anti-human von Willebrand factor antigen (both from Dako) and rat anti-murine CD-34 antigen (Abcam). Sections were pretreated with microwave antigen retrieval in 10 mM citrate buffer for 10 min. Endogenous antibodies were blocked with normal goat serum (1:10 dilution (Vector Laboratories) and then were incubated with the primary antibody localized using an avidin–biotin complex kit (Vector Laboratories) appropriate for the primary antibody. A red alkaline phosphatase substrate was used to avoid confusion with melanin granules.

Assessment of Angiogenesis Rates Within Metastatic Tumors. Intratumoral blood vessels were quantitated using anti-von Willebrand's factor staining, as previously described (17). Intratumoral blood vessels also were assessed by immunoreactivity to CD34, using criteria previously described (19).

Assessment of Apoptosis and Mitosis Rates Within Metastatic Tumors. Mitotic and apoptotic figures were counted on 4-μm H&E-stained slides with a conventional light microscope. Apoptotic bodies (21) were counted, and apoptotic rates were calculated as previously described. For determination of K_i-67 positivity, individual K_i-67 positively stained cells within grid spaces completely occupied by tumor were counted (≈40 grids per lung) and were expressed as the mean number of K_i-67–positive cells per 100 μm^2 of tumor tissue.

Statistical Methods. For continuous, normally distributed data, a one-way ANOVA was used to determine whether there were any differences among different treatments. If this test was significant ($P < 0.05$), pairwise two-sided Student's t tests were conducted to compare the different treatments. This method was used to avoid inflation of P values by multiple testing. When measurements were not normally distributed, a Kruskal–Wallis rank test was used first to test whether there were differences among different treatments (including no treatment). If the Kruskal–Wallis test was significant ($P < 0.05$), the Mann–Whitney rank test was used for comparisons between pairs of treatments. Statistical calculations were carried out using Stata version 11.1 (StataCorp).

ACKNOWLEDGMENTS. We thank R. Chu, Tri Lu, Wayne Liao, Charles Ma, and Kevin Chen for their experimental assistance and T. Heath, P. Billings, J. Patton, J. Muschler, J. Sabry, S. Mintz, and M. Kope for helpful comments on the manuscript. This work was supported by Department of Defense Grant PR043482 (to H.D.), National Institutes of Health Grants HL079090 (to H.D.), U54RR24379 (to D.L.), CA114337 and CA122947 (to M.K.-S.), and CA109174 (to R.D.), and Genomic Systems.

1. Chambers AF, Groom AC, MacDonald IC (2002) Dissemination and growth of cancer cells in metastatic sites. *Nat Rev Cancer* 2:563–572.
2. Gupta GP, Massagué J (2006) Cancer metastasis: Building a framework. *Cell* 127: 679–695.
3. Liotta LA, Kohn EC (2001) The microenvironment of the tumour-host interface. *Nature* 411:375–379.
4. Woodhouse EC, Chuaqui RF, Liotta LA (1997) General mechanisms of metastasis. *Cancer* 80(8, Suppl):1529–1537.
5. Cameron MD, et al. (2000) Temporal progression of metastasis in lung: Cell survival, dormancy, and location dependence of metastatic inefficiency. *Cancer Res* 60: 2541–2546.
6. Steeg PS (2006) Tumor metastasis: Mechanistic insights and clinical challenges. *Nat Med* 12:895–904.
7. O'Brien CD, Cao G, Makrigiannakis A, DeLisser HM (2004) Role of immunoreceptor tyrosine-based inhibitory motifs of PECAM-1 in PECAM-1-dependent cell migration. *Am J Physiol Cell Physiol* 287:C1103–C1113.
8. Yan HC, et al. (1995) Alternative splicing of a specific cytoplasmic exon alters the binding characteristics of murine platelet/endothelial cell adhesion molecule-1 (PECAM-1). *J Biol Chem* 270:23672–23680.
9. Muller WA (1995) The role of PECAM-1 (CD31) in leukocyte emigration: Studies in vitro and in vivo. *J Leukoc Biol* 57:523–528.
10. Newman PJ, Newman DK (2003) Signal transduction pathways mediated by PECAM-1: New roles for an old molecule in platelet and vascular cell biology. *Arterioscler Thromb Vasc Biol* 23:953–964.
11. Kashani-Sabet M, et al. (2002) Identification of gene function and functional pathways by systemic plasmid-based ribozyme targeting in adult mice. *Proc Natl Acad Sci USA* 99:3878–3883.
12. Vantyghem SA, Postenka CO, Chambers AF (2003) Estrous cycle influences organ-specific metastasis of B16F10 melanoma cells. *Cancer Res* 63:4763–4765.
13. Zhou Z, Christofidou-Solomidou M, Garlanda C, DeLisser HM (1999) Antibody against murine PECAM-1 inhibits tumor angiogenesis in mice. *Angiogenesis* 3:181–188.
14. Cao G, et al. (2009) Angiogenesis in platelet endothelial cell adhesion molecule-1-null mice. *Am J Pathol* 175:903–915.
15. DeLisser HM, et al. (1997) Involvement of endothelial PECAM-1/CD31 in angiogenesis. *Am J Pathol* 151:671–677.
16. Tasaka S, et al. (2003) Platelet endothelial cell adhesion molecule-1 in neutrophil emigration during acute bacterial pneumonia in mice and rats. *Am J Respir Crit Care Med* 167:164–170.
17. Liu Y, et al. (1999) Systemic gene delivery expands the repertoire of effective antiangiogenic agents. *J Biol Chem* 274:13338–13344.
18. Nico B, et al. (2008) Evaluation of microvascular density in tumors: Pro and contra. *Histol Histopathol* 23:601–607.
19. Weidner N, Carroll PR, Flax J, Blumenfeld W, Folkman J (1993) Tumor angiogenesis correlates with metastasis in invasive prostate carcinoma. *Am J Pathol* 143:401–409.
20. Werner N, et al. (2005) Circulating endothelial progenitor cells and cardiovascular outcomes. *N Engl J Med* 353:999–1007.
21. van Diest PJ, Brugal G, Baak JP (1998) Proliferation markers in tumours: Interpretation and clinical value. *J Clin Pathol* 51:716–724.
22. Duncan GS, et al. (1999) Genetic evidence for functional redundancy of platelet/endothelial cell adhesion molecule-1 (PECAM-1): CD31-deficient mice reveal PECAM-1-dependent and PECAM-1-independent functions. *J Immunol* 162:3022–3030.
23. Mahooti S, et al. (2000) PECAM-1 (CD31) expression modulates bleeding time in vivo. *Am J Pathol* 157:75–81.
24. Vailhé B, Vittet D, Feige JJ (2001) In vitro models of vasculogenesis and angiogenesis. *Lab Invest* 81:439–452.
25. Malorny U, Michels E, Sorg C (1986) A monoclonal antibody against an antigen present on mouse macrophages and absent from monocytes. *Cell Tissue Res* 243: 421–428.
26. Adams GP, Weiner LM (2005) Monoclonal antibody therapy of cancer. *Nat Biotechnol* 23:1147–1157.
27. Ferrara N (2005) VEGF as a therapeutic target in cancer. *Oncology* 69(Suppl 3):11–16.
28. Podsypanina K, et al. (2008) Seeding and propagation of untransformed mouse mammary cells in the lung. *Science* 321:1841–1844.